

Computational aberration compensation by coded-aperture-based correction of aberration obtained from optical Fourier coding and blur estimation: supplementary material

JAEBUM CHUNG^{1,*}, GLORIA W. MARTINEZ², KAREN C. LENCIONI², SRINIVAS R. SADDA³, AND CHANGHUEI YANG¹

¹Department of Electrical Engineering, California Institute of Technology, Pasadena, CA 91125, USA

²Office of Laboratory Animal Resources, California Institute of Technology, Pasadena, CA 91125, USA

³Doheny Eye Institute, University of California - Los Angeles, Los Angeles, CA 90033, USA

*Corresponding author: jaebum@alumni.caltech.edu

Published 10 May 2019

This document provides supplementary information to “Computational aberration compensation by coded-aperture-based correction of aberration obtained from optical Fourier coding and blur estimation,” <https://doi.org/10.1364/OPTICA.6.000647>.

1. MATHEMATICAL DERIVATION OF CAPTURING IMAGES WITH PUPIL PLANE MODULATION

We consider a point on the unknown sample, $s(x, y)$, and how it propagates to the camera plane to be imaged. On the sample plane, a point source at (x_0, y_0) may have an amplitude and phase C , and it can be described by:

$$U_0(x, y; x_0, y_0) = C\delta(x - x_0, y - y_0) \quad (\text{S1})$$

We then use Fresnel propagation:

$$\begin{aligned} U_1(u, v; x_0, y_0) &= \frac{\exp\left[j\frac{\pi}{\lambda f_0}(u^2 + v^2)\right]}{j\lambda f_0} \int_{-\infty}^{\infty} C\delta(x - x_0, y - y_0) \\ &\exp\left[j\frac{\pi}{\lambda f_0}(x^2 + y^2)\right] \exp\left[-j\frac{2\pi}{\lambda f_0}(xu + yv)\right] dx dy \\ &= C \frac{\exp\left[j\frac{\pi}{\lambda f_0}(u^2 + v^2)\right]}{j\lambda f_0} \exp\left[j\frac{\pi}{\lambda f_0}(x_0^2 + y_0^2)\right] \\ &\exp\left[-j\frac{2\pi}{\lambda f_0}(x_0 u + y_0 v)\right] \end{aligned} \quad (\text{S2})$$

and apply the phase delay associated with an idealized thin lens [1] having an estimated focal length f_0 for the unknown

lens, $\exp\left[-j\frac{\pi}{\lambda f_0}(u^2 + v^2)\right]$, and any discrepancy from the ideal is incorporated into the pupil function, $P(u, v; x_0, y_0) = P_t(u, v)$, where $t = 0$ is the isoplanatic patch around (x_0, y_0) :

$$\begin{aligned} U_2(u, v; x_0, y_0) &= \frac{C}{j\lambda f_0} \exp\left[j\frac{\pi}{\lambda f_0}(x_0^2 + y_0^2)\right] \exp\left[-j\frac{2\pi}{\lambda f_0}(x_0 u + y_0 v)\right] P_t(u, v) \\ &= C_2(x_0, y_0) P_t(u, v) \exp\left[-j\frac{2\pi}{\lambda f_0}(x_0 u + y_0 v)\right] \end{aligned} \quad (\text{S3})$$

where we set $C_2(x_0, y_0) = C/(j\lambda f_0) \exp[j\pi/(\lambda f_0)(x_0^2 + y_0^2)]$. Eq. (S3) is Eq. (2) of the main article.

$U_2(u, v; x_0, y_0)$ is relayed to the pupil plane in Fig. 1 without any additional phase term by the 4f system formed by L1 and L2 [1]. The relayed field may be magnified by the factor f_2/f_1 , but here we assume no magnification. We apply a mask, $M(u, v)$, to the field:

$$\begin{aligned} U_2'(u, v; x_0, y_0) &= M(u, v) C_2(x_0, y_0) P_t(u, v) \exp\left[-j\frac{2\pi}{\lambda f_0}(x_0 u + y_0 v)\right] \end{aligned} \quad (\text{S4})$$

and propagate it by distance d using angular spectrum to the

surface of L3:

$$U_3(s, t; x_0, y_0) = \mathcal{F}^{-1} \{ \mathcal{F} \{ U_2'(u, v; x_0, y_0) \} \exp \left[-j \frac{2\pi d}{\lambda} \sqrt{1 - (\lambda f_x)^2 - (\lambda f_y)^2} \right] \} (s, t) \quad (S5)$$

where (s, t) are the coordinates on the L3's plane. We then apply the phase delay associated with L3, $\exp \left[-j \frac{\pi}{\lambda f_3} (s^2 + t^2) \right]$, and propagate the field by f_3 to the camera plane:

$$\begin{aligned} & U_4(\xi, \eta; x_0, y_0) \\ &= \frac{\exp \left[j \frac{\pi}{\lambda f_3} (\xi^2 + \eta^2) \right]}{j \lambda f_3} \int_{-\infty}^{\infty} \exp \left[-j \frac{\pi}{\lambda f_3} (s^2 + t^2) \right] \\ & U_3(s, t; x_0, y_0) \exp \left[j \frac{\pi}{\lambda f_3} (s^2 + t^2) \right] \exp \left[-j \frac{2\pi}{\lambda f_3} (s\xi + t\eta) \right] ds dt \\ &= \frac{\exp \left[j \frac{\pi}{\lambda f_3} (\xi^2 + \eta^2) \right]}{j \lambda f_3} \int_{-\infty}^{\infty} \mathcal{F}^{-1} \{ \mathcal{F} \{ U_2'(u, v; x_0, y_0) \} \} \\ & \exp \left[-j \frac{2\pi d}{\lambda} \sqrt{1 - (\lambda f_x)^2 - (\lambda f_y)^2} \right] (s, t) \\ & \exp \left[-j \frac{2\pi}{\lambda f_3} (s\xi + t\eta) \right] ds dt \quad (S6) \end{aligned}$$

Set $C_4(\xi', \eta') = \exp [j\pi\lambda f_3(\xi'^2 + \eta'^2)] / (j\lambda f_3)$ and $(\xi', \eta') = (\xi, \eta) / (\lambda f_3)$:

$$\begin{aligned} & U_4'(\xi', \eta'; x_0, y_0) \\ &= C_4(\xi', \eta') \mathcal{F} \{ \mathcal{F}^{-1} \{ \mathcal{F} \{ U_2'(u, v; x_0, y_0) \} \} \} \\ & \exp \left[-j \frac{2\pi d}{\lambda} \sqrt{1 - (\lambda f_x)^2 - (\lambda f_y)^2} \right] (\xi', \eta') \\ &= C_4(\xi', \eta') \mathcal{F} \{ U_2'(u, v; x_0, y_0) * \\ & \mathcal{F}^{-1} \{ \exp \left[-j \frac{2\pi d}{\lambda} \sqrt{1 - (\lambda f_x)^2 - (\lambda f_y)^2} \right] \} \} (\xi', \eta') \\ &= C_4(\xi', \eta') \mathcal{F} \{ U_2'(u, v; x_0, y_0) \} (\xi', \eta') \\ & \exp \left[-j \frac{2\pi d}{\lambda} \sqrt{1 - (\lambda \xi')^2 - (\lambda \eta')^2} \right] \\ &= C_4(\xi', \eta') \exp \left[-j \frac{2\pi d}{\lambda} \sqrt{1 - (\lambda \xi')^2 - (\lambda \eta')^2} \right] \\ & \mathcal{F} \{ M(u, v) C_2(x_0, y_0) P_t(u, v) \exp \left[-j \frac{2\pi}{\lambda f_0} (x_0 u + y_0 v) \right] \} (\xi', \eta') \quad (S7) \end{aligned}$$

where $*$ is the convolution operator.

Set $C_4(\xi', \eta') \exp \left[-j \frac{2\pi d}{\lambda} \sqrt{1 - (\lambda \xi')^2 - (\lambda \eta')^2} \right] C_2(x_0, y_0)$ as $C_5(\xi', \eta'; x_0, y_0)$:

$$\begin{aligned} & U_4'(\xi', \eta'; x_0, y_0) \\ &= C_5(\xi', \eta'; x_0, y_0) \mathcal{F} \{ M(u, v) P_t(u, v) \} (\xi', \eta') \\ & * \delta \left(\xi' + \frac{x_0}{\lambda f_0}, \eta' + \frac{y_0}{\lambda f_0} \right) \\ &= C_5(\xi', \eta'; x_0, y_0) \mathcal{F} \{ M(u, v) P_t(u, v) \} \left(\xi' + \frac{x_0}{\lambda f_0}, \eta' + \frac{y_0}{\lambda f_0} \right) \quad (S8) \end{aligned}$$

This is the complex field incident on the camera from the point source located at (x_0, y_0) . It is the PSF of the system, and we observe that it simply shifts laterally for different (x, y) coordinates. Therefore, the image on the camera sensor can be

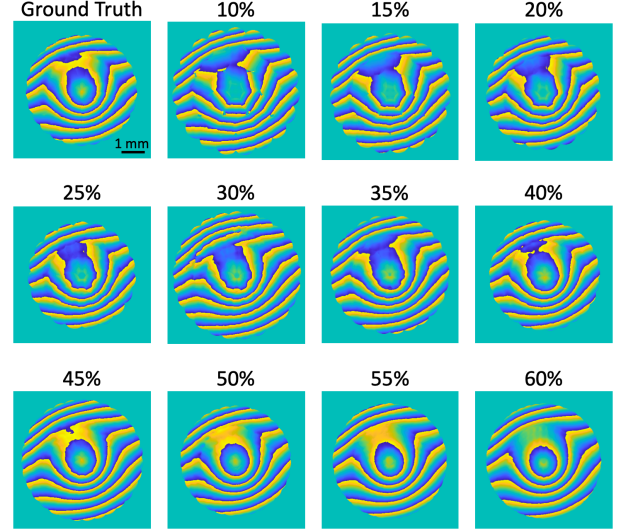


Fig. S1. The influence of the limited masks' overlap ratio on the pupil function recovery. The recovery becomes poor below 30% overlap.

calculated by a convolution between $U_4'(\xi', \eta'; x_0, y_0)$ and the sample field within the isoplanatic patch, $s_t(x, y)$. However, the phase term in $C_5(\xi', \eta'; x_0, y_0)$ can have a significant impact on the captured images. In our incoherent imaging scenario, the phase relationship between the points on the sample plane during the capturing process is irrelevant. So, we can define an intensity PSF, $h_t(\xi, \eta) = |\mathcal{F} \{ M(u, v) P_t(u, v) \}(\xi, \eta)|^2$, to describe the intensity of the $U_4'(\xi', \eta'; x_0, y_0)$ captured by the camera:

$$\begin{aligned} & |U_4'(\xi', \eta'; x_0, y_0)|^2 \\ &= |C_5(\xi', \eta'; x_0, y_0)|^2 h_t \left(\xi' + \frac{x_0}{\lambda f_0}, \eta' + \frac{y_0}{\lambda f_0} \right) \\ &= \frac{C}{\lambda^2 f_0 f_3} h_t \left(\xi' + \frac{x_0}{\lambda f_0}, \eta' + \frac{y_0}{\lambda f_0} \right) \quad (S9) \end{aligned}$$

The complicated phase fluctuations embedded in $C_5(\xi', \eta'; x_0, y_0)$ become no longer relevant. Dropping the constants and neglecting coordinate scaling, the image of the unknown sample captured by the camera becomes a convolution of $h_t(\xi, \eta)$ with the sample distribution, s_t , as described by Eq. (5) of the main article.

2. LIMITED APERTURE OVERLAP REQUIREMENT FOR PUPIL FUNCTION RECONSTRUCTION

Given the ground truth pupil function 5 mm in diameter and the limited mask diameter of 1 mm, the area overlap between contiguous masks are varied from 10% to 60% in simulation. In spatial domain, all images are captured satisfying the Nyquist criterion. The simulation is identical to Fig. 6's data acquisition and reconstruction using Algorithm 1 and 2. As shown in Fig. S1, the recovery becomes poor below 30% overlap as observed by disconnected fringe patterns, and eventually contains holes in regions where there was no masks' coverage.

3. INCREASING SNR BY AVERAGING OVER MULTIPLE FRAMES

In processing the data from the in-vivo experiment, motion-reference camera images are first registered for rotation and

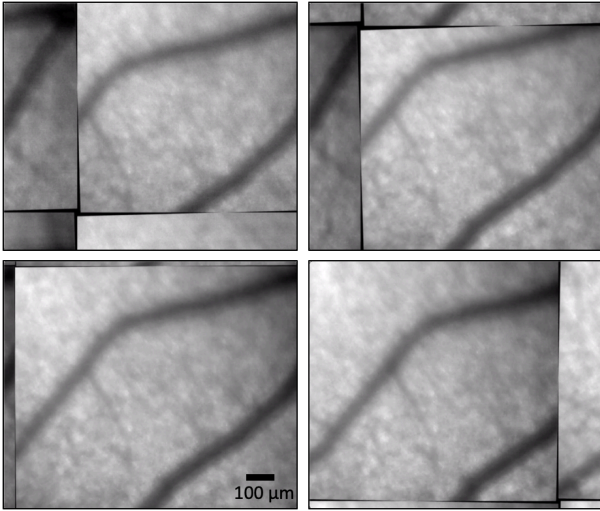


Fig. S2. Motion-reference camera images registered for rotation and translation (see **Visualization 1**).

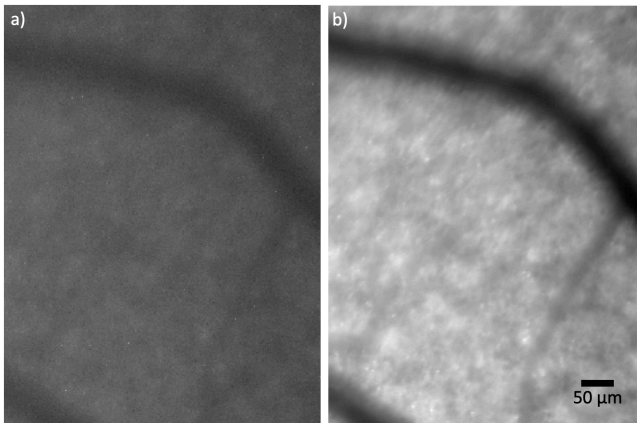


Fig. S3. Raw full aperture image. a) 1 frame and b) a sum of 213 frames.

translation, as shown in Fig. S2 and **Visualization 1**, and these registration values are taken into account when summing multiple frames captured with the same SLM aperture pattern.

An example of a single frame of full aperture image is shown in Fig. S3, and the same aperture image after summing 213 frames.

Due to the photon-starved imaging condition, it is imperative to account for the detector noise in the captured images. We use two-point radiometric calibration to account for the fixed pattern noise and inhomogeneous sensitivity of our imaging sensor [2]:

$$I'(\xi, \eta) = \frac{I(\xi, \eta) - B(\xi, \eta)}{R(\xi, \eta) - B(\xi, \eta)} \quad (\text{S10})$$

where (ξ, η) are the coordinates on the camera sensor's plane, $I'(\xi, \eta)$ is the desired calibrated image, $I(\xi, \eta)$ is the input image, $B(\xi, \eta)$ is the dark image captured with the sensor blocked from light, and $R(\xi, \eta)$ is a reference image captured with the sensor capturing an image of an opal diffuser.

REFERENCES

1. J. Goodman, *Introduction to Fourier Optics* (McGraw-Hill, 2008).
2. B. Jähne, *Digital Image Processing* (Springer, 2005).